Vysoká škola báňská - Technická univerzita Ostrava, Univerzitní studijní program Nanotechnologie / VŠB-TUO, University Programme: Nanotechnology

Optická a magneto-optická spektrální elipsometrie tenkých vrstev a nanostruktur /Optical and Magneto-optical Spectral Ellipsometry of Thin Films and Nanostructures

Ondřej Vlašín
Thesis Supervisor: Ing. David Hrabovský, PhD.

2009

Contents

Nomenclature

$r_{s,p}$ intensity of reflected wave in s and p polarization, page 14

β_0 amplitude of Faraday cell azimuth modulation in radians, page 35

χ_p Fresnel coefficients or the complex Kerr effects for p-polarized incident beam, page 11

χ_s Fresnel coefficients or the complex Kerr effects for s-polarized incident beam, page 11

χ_t transverse complex Kerr effect, page 11

† Hermitian adjoint, page 17

Δn is change of index of refraction in saturated state, page 14

δ phase-plate phaseshift, page 35

$\epsilon_{p/s}$ Kerr ellipticity, page 12

η azimuth of compensating Faraday cell, page 35

Γ modulated part of electric field, page 16

γ retardation angle of the compensator, page 10

Γ^* additive inverse of complex number Γ, page 17

$\mathbb{A}$ matrix representation of analyzer, page 10

$\mathbb{C}$ tranformation matrix for lineary polarized light propagating through compensator, page 10

$\mathbb{G}_{ab}$ matrix representation of two polarizers with azimuths a and b, page 11

$\mathbb{M}$ modulator matrix, page 10

$\mathbb{P}$ matrix representation of polarizer, page 10

$\mathbb{R}$ rotation matrix, page 10

$\mathbb{S}$ Johnson matrix of sample, page 11

$\mathbf{E_{out}}$ electric field at the detector, page 17

$\mathbf{E_{in}}$ incident electric field, page 17

$\mathbf{J}_n(\alpha)$ value of Bessel function of the first kind and n-th order at α, page 17

ω frequency, page 10

Ω_x functions of setup geometry, page 18

ψ, Δ ellipsometric angles defined as $\frac{r_{pp}}{r_{ss}} = \tan\psi e^{-i\Delta}$, where r_{pp} and r_{ss} are Fresnel coefficients for p and s polarizations, page 12

$\theta_{p/s}$ Kerr rotation, page 12

φ modulation depth of the P.E.M., page 10

φ_0 residual birefringence, page 10

φ_A amplitude of modulation, page 10

$C(\Delta)$ real part of phase shift upon reflection with transversal Kerr effect (it converges to $\cos\Delta$ for $\chi_t \to 0$), page 12

E electric field, page 13

H magnetic field, page 13

I electric field intensity, page 17

I_0 unmodulated part of field intensity, page 17

$I_{2\omega}$ second harmonic part of field intensity, page 17

Abstract This work is revolving around ellipsometry and its applications in magneto-optics. Ellipsometry is particularly attractive for its suitability for *in-situ* measurements and remarkable sensitivity to minute inter-facial effects, such as the formation of sub-mono-layer of atoms or magneto-optical (MO) effect. Special attention is given to ellipsometric setups with photo-elastic modulator (**PEM**) that are favored for its high signal to noise ratio.

Common way of obtaining equations for analysis of spectroscopic data is a direct derivation from Jones or Mueller matrices of the system for each configuration separately. In spite of its various advantages general equation of ellipsometric setup are not being used. For this reason general scalar equations for **PEM** (photo-elastic modulator) based ellipsometric measurements are derived here that allow easy calculation of each component's imperfection influence on the results as well as quick insight to all configurations possible. Along with general equation a simplification to Jones Formalism that optimizes numerical calculation is proposed.
The spectral magneto-optical measurements of polar, longitudinal and transverse Kerr effect are analyzed with photo-elastic and Faraday cell modulation.

Based on the general equation a nulling method for **MOKE** (magneto-optical Kerr Effect) measurements is calculated and experimentally verified that offers above average precision in desired region of measurement and reduces moving parts to a single branch of the measurement setup further improving noise cancellation possibilities. The trade-off of the proposed method is slightly more complicated nulling procedure.

Furthermore an automatic calibration of spectral MOKE measurement setup was designed, programed and applied. For simulation and data analysis a Yeh formalism based program was developed with few applications presented here.

The need for fast and precise magneto-optic measurements has been steadily growing since the discovery of the giant magneto resistive (GMR) effect in 1988 [BBF$^+$88]. A new technology, called spintronics, has emerged [WAB$^+$01]. In spintronics, the logical information is carried by spins of electrons or nuclei in addition to, or instead of, their charge. The first practical spintronic devices have been GMR based read heads for magnetic hard drives, announced by IBM in 1997. Another major technological breakthrough is anticipated to come from nonvolatile magnetic random access memories (MRAMs) [Dax97].

Keywords Kerr effect, MOKE, ellipsometry, Faraday cell, azimuth modulation, photo-elastic modulator calibration

Scope of Thesis The aim of this thesis is an improvement of ellipsometric measurements of magneto-optical Kerr effect in both theoretical and practical point of view.

Part I introduces general equation for ellipsometric setups with photo-elastic modulator (PEM). All possible measurement configurations are analyzed. A novel method that promises above average precision in desired region of measurement and enables further improvement of noise cancellation is presented.

In chapter 4 calibration method for PEM based magneto-optic Kerr effect (MOKE) measurement setups is presented along with result of its practical application.

Chapter 5 shows few examples of spectral MOKE simulations using Yeh formalism based program developed by the author of this work.

In the third part various modulation techniques for MOKE measurements are compared. The most promising method is proposed for application based on signal-to-noise-ratio analysis.

Fourth part summarizes the results of this thesis and outlines the future development and aims.

Part I.

General Equation

Chapter 1.

Jones Formalism

In this work I will use Jones 2×2 formalism for Kerr effect analysis and Yeh formalism according to [Yeh80] for more detailed sample analysis and modeling. General non-matrix theories are cited from [ST95].

Propagation of electromagnetic wave through any optical component can be described by transformation matrix of electromagnetic field vector. Each optical device is being assigned Jones 2×2 matrix as follows [BW75][YY84]

$$\mathbb{A} = \mathbb{P} = \begin{bmatrix} 1 & 0 \\ 0 & 0 \end{bmatrix} \mathbb{C}(\gamma) = \begin{bmatrix} 1 & 0 \\ 0 & \mathrm{e}^{-\mathrm{i}\gamma} \end{bmatrix} \tag{1.1}$$

$$\mathbb{M}(\varphi) = \begin{bmatrix} 1 & 0 \\ 0 & \mathrm{e}^{-\mathrm{i}\varphi} \end{bmatrix} \tag{1.2}$$

where γ is the retardation angle of the compensator and $\varphi = \varphi_0 + \varphi_A \sin \omega t$ is the periodic retardation angle of the photo-elastic modulator (PEM) with the modulation frequency ω, amplitude φ_A and DC signal φ_0. $\mathbb{P}$ and $\mathbb{A}$ stand for polarizer and analyzer. $\mathbb{M}$ is matrix of modulator, $\mathbb{C}$ is matrix of compensator.
The rotation of the components is described by the rotation matrix

$$\mathbb{R}_a = \begin{bmatrix} \cos a & \sin a \\ -\sin a & \cos a \end{bmatrix}, \tag{1.3}$$

so that the analyzer rotated at the azimuth angle a

$$\mathbb{A}_a = \mathbb{R}_{-a}\mathbb{A}\mathbb{R}_a = \begin{bmatrix} \cos^2 a & \sin a \cos a \\ \sin a \cos a & \sin^2 a \end{bmatrix}. \tag{1.4}$$

1.1. Symmetrical Simplification

Further simplification of the formalism can be achieved by splitting compensator and modulator matrices into pair of simultaneous polarizers, where the second

polarizer is shifted by $\frac{\pi}{2}$ in azimuth and introduces the modulation to the signal.

$$\begin{aligned}\mathbb{M}_{\varphi m} = &\begin{bmatrix} \cos^2 m & \cos m \sin m \\ \cos m \sin m & \sin^2 m \end{bmatrix} \\ &+ \mathrm{e}^{-\mathrm{i}\varphi} \begin{bmatrix} \sin^2 m & -\cos m \sin m \\ -\cos m \sin m & \cos^2 m \end{bmatrix} \\ &= \mathbb{A}_m + \mathrm{e}^{-\mathrm{i}\varphi} \mathbb{A}_{m+\pi/2} \end{aligned} \quad (1.5)$$

Here m stands for azimuth angle of modulator. Having done this, the general equation of the system can be derived using few simple mathematical operations:

$$\mathbb{P}_a \mathbb{S} \mathbb{P}_b = (S \cdot G_{ab}) \mathbb{G}_{ab} \quad (1.6)$$

$$\mathbb{G}_{ab} = \begin{bmatrix} \cos a \cos b & \sin b \cos a \\ \sin a \cos b & \sin b \sin a \end{bmatrix} \quad (1.7)$$

$$\mathbb{A} \mathbb{R}_a \mathbb{G}_{cm} \mathbb{R}_{-p} \mathbb{P} = \cos(a-c) \cdot \cos(m-p) \mathbb{P} \quad (1.8)$$

where $\mathbb{G}_{ab}$ is matrix representation of 2 polarizers with azimuth angles a and b.

This simplification as you can see in eq. 1.8 reduces matrices variety in the calculation to polarizer only, which significantly speeds up numerical calculations.

1.2. Sample Representation

The Fresnel coefficients give the ratio of the reflected and transmitted electric field amplitude to initial electric field for electromagnetic radiation incident on a dielectric. In general, when a wave reaches a boundary between two different dielectric constants, part of the wave is reflected and part is transmitted, with the sum of the energies in these two waves equal to that of the original wave. Since electromagnetic waves are transverse, there are separate coefficients in the directions perpendicular to and parallel to the surface of the dielectric. The coefficient for reflection of the "transverse electric field" (abbreviated "TE") is denoted r_{ss}, while the coefficient for reflection of the "transverse magnetic field" (abbreviated "TM") is denoted r_{pp} .

The sample can be represented either using the mentioned Fresnel coefficients or the complex Kerr effects for s-polarized (TE) incident beam (χ_s) and for p-polarized (TM) incident beam (χ_p) and transverse complex Kerr effect χ_t:

$$\mathbb{S} = \begin{bmatrix} r_{ss} & r_{ps}(M_P, M_L) \\ r_{sp}(M_P, M_L) & r_{pp}(M_T) \end{bmatrix} \quad (1.9)$$

$$= r_{ss} \begin{bmatrix} 1 & \chi_s \\ -\chi_p \rho' & \rho' \end{bmatrix} \quad (1.10)$$

where $M_{P,L,T}$ stands for polar, longitudinal and transverse magnetization. Complex Kerr effects are defined as

$$\chi_s = \frac{r_{ps}}{r_{ss}} = \theta_s + \mathrm{i}\epsilon_s \tag{1.11}$$

$$\chi_p = -\frac{r_{sp}}{r_{pp}} = \theta_p + \mathrm{i}\epsilon_p \tag{1.12}$$

$$\chi_t = \theta_t + \mathrm{i}\epsilon_t = 2\delta\psi \csc 2\psi + \mathrm{i}\delta\Delta, \tag{1.13}$$

where $\theta_{p/s}$ is Kerr rotation and $\epsilon_{p/s}$ Kerr ellipticity in p and s polarization. The transverse effect is defined as a small perturbation of ellipsometric angles ψ and Δ with following approximations:

$$\exp\left[\mathrm{i}(\Delta + \delta\Delta)\right] \approx \exp[\mathrm{i}\Delta]\,(1 + \mathrm{i}\delta\Delta) \tag{1.14}$$

$$\tan(\psi + \delta\psi) \approx \tan\psi(1 + 2\delta\psi \csc 2\psi). \tag{1.15}$$

With $\rho = \frac{r_{pp}}{r_{ss}} = \tan\psi \mathrm{e}^{-\mathrm{i}\Delta}$ we can write

$$\rho' = \rho\,(1 + \chi_t) = \tan\psi\,[C(\Delta) + \mathrm{i}S(\Delta)]\,, \tag{1.16}$$

where

$$C(\Delta) = \cos\Delta\,(1 + \theta_t) - \epsilon_t \sin\Delta \tag{1.17}$$

$$S(\Delta) = \epsilon_t \cos\Delta + \sin\Delta\,(1 + \theta_t)\,. \tag{1.18}$$

Sample representation with complex Kerr effect is better suited for general equation derivation as it exploits the symmetry of the three Kerr effects.

Chapter 2.

Yeh Formalism

For Maxwell equations

$$\nabla \times \mathbf{H} = \varepsilon \frac{\partial \mathbf{E}}{\partial t} \tag{2.1}$$

$$\nabla \times \mathbf{E} = -\mu \frac{\partial \mathbf{H}}{\partial t} \tag{2.2}$$

where **E** is time dependent electric field and **H** is time dependent magnetic field with phase $\omega t - \mathbf{k}.\mathbf{r}$ (**k** ...wave vector, **r**...space vector, ω...frequency,t...time) we can write

$$\begin{aligned} \mathbf{k} \times \mathbf{E} &= \omega \mu \mathbf{H} \\ \mathbf{k} \times \mathbf{H} &= -\omega \varepsilon \mathbf{E} \end{aligned}$$

and eliminating **H**

$$\mathbf{k} \times (\mathbf{k} \times \mathbf{E}) + \omega^2 \varepsilon \mu \mathbf{E} = 0 \tag{2.3}$$

which can be rewritten in a matrix form

$$\begin{bmatrix} \varepsilon_{xx} - N_y^2 - N_z^2 & \varepsilon_{xy} & \varepsilon_{xz} \\ \varepsilon_{yx} & \varepsilon_{yy} - N_z^2 & \varepsilon_{yz} + N_y N_z \\ \varepsilon_{zx} & \varepsilon_{zy} + N_y N_z & \varepsilon_{zz} - N_y^2 \end{bmatrix} \begin{bmatrix} e_x \\ e_y \\ e_z \end{bmatrix} = 0 \tag{2.4}$$

where ε_{ij} are elements of permittivity tensor. $e_x, e_y$and e_z are components of electromagnetic field vector. Propagation vector is represented by its component

parallel to the surface (N_y) and its component perpendicular to the surface (N_z) according to fig. 2.1.

Yeh matrix formalism is very useful in the calculation of the reflectance and transmittance of an anisotropic layered medium. There are four complex amplitudes associated with the reflection and another four associated with the transmission. These eight complex amplitudes can be expressed in terms of the matrix elements of the overall transfer matrix. Let i_s be the TE incident wave, r_s the TE reflected wave and t_s the TE transmitted wave and i_p,r_p and t_p the same for TM configuration. Using transfer matrix $\mathbb{M}$ we can write

$$\begin{pmatrix} i_s \\ r_s \\ i_p \\ r_p \end{pmatrix} = \mathbb{M} \begin{pmatrix} t_s \\ 0 \\ t_p \\ 0 \end{pmatrix} \tag{2.5}$$

Fresnel coefficient can be expressed as follows. Coefficient r_{ss} is defined as a ratio of amplitude of reflected wave in s polarization to amplitude of incident wave in s polarization assuming ideally polarized incident wave ($i_p = 0$)

$$\begin{aligned} i_s &= t_s M_{11} + t_p M_{13} \\ r_s &= t_s M_{21} + t_p M_{23} \\ i_p &= t_s M_{31} + t_p M_{33} \end{aligned} \tag{2.6}$$

Eliminating t_s by the third equation we can write

$$r_{ss} = \left(\frac{r_s}{i_s}\right)_{i_p=0} = \frac{M_{33}M_{21} - M_{23}M_{31}}{M_{33}M_{11} - M_{13}M_{31}} \tag{2.7}$$

and analogically for all remaining coefficients.

Anisotropy induced by magnetic field is represented by Voigt parameter defined as

$$Q = \frac{2\Delta n}{n}, \tag{2.8}$$

where n is the index of refraction and Δn is change of index of refraction in saturated state. With different direction of magnetization the permittivity tensor can be expressed as

$$\varepsilon_{polar} = \varepsilon \begin{pmatrix} 1 & -jQ & 0 \\ jQ & 1 & 0 \\ 0 & 0 & 1 \end{pmatrix} \tag{2.9}$$

$$\varepsilon_{longitudinal} = \varepsilon \begin{pmatrix} 1 & 0 & jQ \\ 0 & 1 & 0 \\ -jQ & 0 & 1 \end{pmatrix} \tag{2.10}$$

$$\varepsilon_{transversal} = \varepsilon \begin{pmatrix} 1 & 0 & 0 \\ 0 & 1 & -jQ \\ 0 & jQ & 1 \end{pmatrix} \tag{2.11}$$

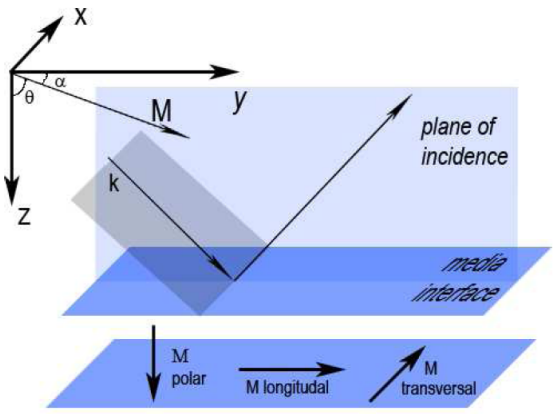

Figure 2.1.: Directions of magnetization

Chapter 3.

General Ellipsometric Equation

In this chapter general equation for ellipsometric measurements is derived for purpose of determining each component's imperfection influence on the results as well as quick insight to all configurations possible. In the second part of this chapter various nulling procedures are described. Nulling is a procedure where by adjusting the component geometry, zero signal is obtained at the detector. There are two main advantages of nulling. Firstly it reduces photonic noise in measurement of the magneto-optic signal, secondly the signal detected after introduction of magnetic field is then directly proportional to magneto-optic effects.

3.1. PMSCA Measurement Setup

PMSCA = Polarizer-Modulator-Sample-Compensator-Analyzer

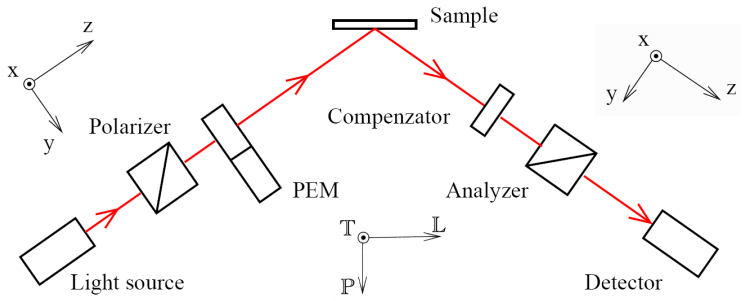

Figure 3.1.: PMSCA setup scheme

If we now make use of (1.8) and split the equation into modulated Γ and unmodulated Γ_0 part

$$\mathbf{E_{out}} = \begin{bmatrix} \Gamma_0 + e^{-i\varphi}\Gamma & 0 \\ 0 & 0 \end{bmatrix} \mathbf{E_{in}} \tag{3.1}$$

$$\begin{aligned}\Gamma_0 = &\quad (S \cdot G_{cm}) \cos(a-c) \cos(p-m) \\ &+ \quad (S \cdot G_{c'm}) \sin(a-c) \cos(p-m) \mathrm{e}^{-\mathrm{i}\gamma} \\ \Gamma = &\quad (S \cdot G_{cm'}) \cos(a-c) \sin(p-m) \\ &+ \quad (S \cdot G_{c'm'}) \sin(a-c) \sin(p-m) \mathrm{e}^{-\mathrm{i}\gamma}\end{aligned}$$

where $\mathbf{E_{in}}$ is incident electric field and $\mathbf{E_{out}}$ is electric field at the detector.

Using Hermitian ad-joint † the intensity of the field can be calculated as

$$\begin{aligned} I &= \mathbf{E}^\dagger \mathbf{E} = (\Gamma_0 + \mathrm{e}^{-\mathrm{i}\varphi}\Gamma)^*(\Gamma_0 + \mathrm{e}^{-\mathrm{i}\varphi}\Gamma) \\ &= |\Gamma_0|^2 + |\Gamma|^2 + 2\cos\varphi \Re\{\Gamma\Gamma_0^*\} + 2\sin\varphi \Im\{\Gamma\Gamma_0^*\} \qquad (3.2) \\ &= |\Gamma_0|^2 + |\Gamma|^2 + 2\cos\varphi \Re\{\Gamma_0\Gamma^*\} - 2\sin\varphi \Im\{\Gamma_0\Gamma^*\}. \qquad (3.3)\end{aligned}$$

Using Bessel functions expansion of $\sin(\varphi_0 + \varphi_A \sin\omega t)$ and $\cos(\varphi_0 + \varphi_A \sin\omega t)$

$$\begin{aligned}\sin(\varphi_0 + \varphi_A \sin\omega t) &= \mathrm{J}_0(\varphi_A)\sin\varphi_0 + 2\mathrm{J}_1(\varphi_A)\cos\varphi_0 \sin\omega t \qquad (3.4) \\ &\quad + 2\mathrm{J}_2(\varphi_A)\sin\varphi_0 \cos 2\omega t + ... \\ \cos(\varphi_0 + \varphi_A \sin\omega t) &= \mathrm{J}_0(\varphi_A)\cos\varphi_0 - 2\mathrm{J}_1(\varphi_A)\sin\varphi_0 \sin\omega t \qquad (3.5) \\ &\quad + 2\mathrm{J}_2(\varphi_A)\cos\varphi_0 \cos 2\omega t + ...\end{aligned}$$

we arrive at the general expressions for the first and the second harmonic of the PMSCA ellipsometric setup:

$$I_\omega = -4\mathrm{J}_1(\varphi_A)\left(\cos\varphi_0 \Im\{\Gamma_0\Gamma^*\} + \sin\varphi_0 \Re\{\Gamma_0\Gamma^*\}\right) \qquad (3.6)$$

$$I_{2\omega} = 4\mathrm{J}_2(\varphi_A)\left(\cos\varphi_0 \Re\{\Gamma_0\Gamma^*\} - \sin\varphi_0 \Im\{\Gamma_0\Gamma^*\}\right) \qquad (3.7)$$

For DC (direct current) signal we can write:

$$I_{dc} = |\Gamma_0|^2 + |\Gamma|^2 + 4\mathrm{J}_0(\varphi_A)\left(\cos\varphi_0 \Re\{\Gamma_0\Gamma^*\} - \sin\varphi_0 \Im\{\Gamma_0\Gamma^*\}\right) \qquad (3.8)$$

According to equation (3.3) and (3.2) and assuming negligible residual birefringence:

$$\begin{aligned} I_\omega &= 2\Im\{\Gamma\Gamma_0^*\} = -2\Im\{\Gamma^*\Gamma_0\} \qquad (3.9) \\ I_{2\omega} &= 2\Re\{\Gamma\Gamma_0^*\} = 2\Re\{\Gamma^*\Gamma_0\} \qquad (3.10) \\ I_0 &= |\Gamma_0|^2 + |\Gamma|^2 \qquad (3.11)\end{aligned}$$

To obtain equations for the first and the second harmonic signal intensity it is sufficient to calculate $\Gamma\Gamma_0^*$.

$$\begin{aligned}\frac{\Gamma\Gamma_0^*}{\frac{1}{2}|r_{ss}|^2 \sin_{2(p-m)}} = \quad & (1-\Omega_0)\left(\theta_s \cos 2m - \tfrac{1}{2}\sin 2m + \mathrm{i}\epsilon_s\right) \\ & -\Omega_0 t_\psi^2 \left(\theta_p \cos 2m - \tfrac{1}{2}\sin 2m + \mathrm{i}\epsilon_p\right) \\ +(\Omega_1 - \mathrm{i}\Omega_2)\tan\psi & \left(\tfrac{1}{2}\sin 2m.(X_1 + \mathrm{i}X_2) + \cos^2 m.(C(\Delta) + \mathrm{iS}(\Delta))\right) \\ +(\Omega_1 + \mathrm{i}\Omega_2)\tan\psi & \left(\tfrac{1}{2}\sin 2\mathrm{m}.(X_1 + \mathrm{i}X_2) - \sin^2 m.(C(\Delta) - \mathrm{iS}(\Delta))\right)\end{aligned}$$

where

$$\begin{aligned}2\Omega_0 &= 2 - 2c + \sin 2(a-c)\sin 2c\cos\gamma \\ 2\Omega_1 &= \cos 2(a-c)\sin 2c + \cos 2c \sin 2(a-c)\cos\gamma \\ 2\Omega_2 &= \sin 2(a-c)\sin\gamma\end{aligned}$$

and

$$\begin{aligned}X_1 &= C(\Delta)(\theta_p + \theta_s) + S(\Delta)(\epsilon_s - \epsilon_p) \\ X_2 &= S(\Delta)(\theta_p + \theta_s) - C(\Delta)(\epsilon_s - \epsilon_p).\end{aligned}$$

According to (3.9) and (3.10)

$$\begin{aligned}\frac{I_\omega}{|r_{ss}|^2 \sin 2(p-m)} &= \tan\psi(\Omega_1 S(\Delta) - \Omega_2 C(\Delta)) \\ &\quad -\Omega_0(\epsilon_s + \tan^2\psi\epsilon_p) + \epsilon_s \\ &\quad + \sin 2m\Omega_1 \tan\psi X_2 \qquad (3.12) \\ \frac{I_{2\omega}}{|r_{ss}|^2 \sin 2(p-m)} &= [\tan\psi(\Omega_1 C(\Delta) + \Omega_2 S(\Delta)) \\ &\quad -\Omega_0(\theta_s + \tan^2\psi\theta_p) + \theta_s]\cos 2m \\ &\quad + \sin 2m\Omega_1 \tan\psi X_1 + \sin 2m[\Omega_0 \cos^{-2}\psi - 1] \qquad (3.13)\end{aligned}$$

If we substitute into equation 3.11:

$$\frac{I_0}{\frac{1}{2}|r_{ss}|^2} = \quad \Omega_0 \tan^2\psi + (\Omega_1 X_1 + \Omega_2 X_2)\tan\psi + 1 - \Omega_0 \qquad (3.14)$$

3.2. Nulling

Without magnetic field ($C(\Delta) = \cos\Delta$, $S(\Delta) = \sin\Delta$) we get for the zero of the first harmonic ($I_\omega = 0$)

$$\cot\Delta \;=\; \frac{\Omega_1}{\Omega_2} = \cot 2(a-c)\sin 2c\csc\gamma + \cos 2c\cot\gamma \tag{3.15}$$

and for the second harmonic zero ($I_{2\omega} = 0$)

$$\tan\psi = \pm\sqrt{\alpha^2 - 1 + \Omega_0^{-1}} - \alpha \tag{3.16}$$

$$\alpha = \tfrac{1}{2}\cot 2m\,.\,(\Omega_1\cos\Delta + \Omega_2\sin\Delta)\Omega_0^{-1}. \tag{3.17}$$

Here are some measurement configuration as proposed by [AB87]:

3.2.1. Fixed Compensator Configuration

Plugging $c = (\pm)_c\pi/4$ and $\gamma = \frac{\pi}{2}$ into 3.15 we obtain

$$\cot\Delta = (\mp)_c\cot\left(2a(\pm)_c 2c\right). \tag{3.18}$$

Furthermore, using equality

$$\cot^{-1}(a-b) = \cot^{-1}a + \cot^{-1}[(a^2 - ab + 1)/b]$$

and noting that $\cos(\gamma - \frac{\pi}{2}) \approx \sin\gamma$, as $\gamma \to \frac{\pi}{2}$ we can write

$$\Delta = (\pm)_\Delta(\mp)_c\left(2a(\pm)_c\frac{\pi}{2}\right), \tag{3.19}$$

where $(\pm)_\Delta$ corresponds to periodicity of cotangent.

Imprecision in calculation of Δ can be approximated as

$$\delta\Delta = \delta_a + \delta_c + \delta_\gamma + \cos^2(2a)\delta_c\delta_\gamma, \tag{3.20}$$

where $\delta_c = \frac{\pi}{2} - 2c$ and $\delta_\gamma = \frac{\pi}{2} - \gamma$. δ_γ contains imperfections of the quarter-wave plate and varies with wavelength as $\gamma = \frac{2\pi}{\lambda}|n_e - n_0|d$. For example, effect of using 650 nm laser with a first order quarter wave plate made for 632.8 nm laser ($\delta\gamma = 0.04$) is still negligible. Imprecision in calculation of Δ angle is therefore double the sum of the smallest adjustable azimuth step of compensator and of

analyzer. Smallest adjustable step typically varies from 10 mrad in basic laboratory equipment to 1 mrad in commercial ellipsometres.

Note that the first harmonic signal is independent of modulator azimuth and with the modulator azimuth fixed to $\pm\frac{\pi}{4}$, the second harmonic is independent of Δ.

General equations 3.12 and 3.13 collapse with this configuration to standard pair of equations [PMY+04]

$$\begin{aligned} I_\omega &= \tan\psi(\sin 2a \sin\Delta \pm \cos 2a \cos\Delta \sin\gamma) \\ I_{2\omega} &= \tan\psi \cos 2m(\sin 2a \cos\Delta \mp \cos 2a \sin\Delta \sin\gamma) \\ &+ \tfrac{1}{2}\sin 2m\left[(1+\tan^2\psi)(\cos 2a \cos\gamma) + (1-\tan^2\psi)\right]. \end{aligned} \tag{3.21}$$

Plugging 3.15 into 3.21 we get

$$\begin{aligned} \tan\psi &= (\pm)_\Delta \frac{1}{\tan 2m}(\pm)_\psi \frac{1}{\sin 2m} \\ &= \left\{ \begin{array}{cc|l} \Delta & \psi & \\ \hline + & + & \psi = -m + \pi/2 \\ + & - & \psi = -m \\ - & + & \psi = +m \\ - & - & \psi = +m - \pi/2 \end{array} \right. \end{aligned} \tag{3.22}$$

where $(\pm)_\psi$ corresponds to two roots of the quadratic equation.

3.2.2. Fixed Analyzer Configuration

Similar results can be obtained for fixed analyzer and rotating compensator.

$$\begin{aligned} a = 0, \pm\tfrac{\pi}{2}; I_\omega = 0 &\Rightarrow \tan\Delta = \sec 2c \\ a = \pm\tfrac{\pi}{4}; I_\omega = 0 &\Rightarrow \cot\Delta = \pm\sec 2c \mp \cos 2c \\ a = \pm\tfrac{\pi}{4}; I_{2\omega} = 0 &\Rightarrow \end{aligned}$$

$$\begin{aligned} t_\psi &= \frac{(\pm)_a \cos 2m \sin\Delta \cos 2c(\sin^2 2c \tan^2 2c + 1)}{1(\mp)_a \frac{1}{2}\sin 4c \sin 2m} \\ &\left[-1(\pm)_\psi \sqrt{1 - \frac{\tan^2 2m}{\sin^2\Delta} \frac{3(\mp)_a 2\sin 4c + \frac{1}{4}\sin^2 4c}{\cos^2 2c(\sin^2 2c \tan^2 2c + 1)^2}} \right] \end{aligned} \tag{3.23}$$

3.2.3. Fixed Modulator-Polarizer Configuration

For the simplest configuration without compensator and with polarizer at 45° and modulator at 0°, the above equations collapse to

$$I_{a=0} = |r_{ss}|^2(1 + \theta_s \cos\varphi + \epsilon_s \sin\varphi) \tag{3.24}$$
$$I_{a=\frac{\pi}{2}} = |r_{pp}|^2(1 - \theta_p \cos\varphi + \epsilon_p \sin\varphi) \tag{3.25}$$

If we have modulator azimuth fixed to $\pm\frac{\pi}{4}$ and polarizer azimuth to 0 we obtain for the first and the second harmonic zeros

$$I_\omega \approx I_s = 0 : \tan\Delta = \frac{\Omega_2}{\Omega_1} \tag{3.26}$$
$$I_{2\omega} \approx I_c = 0 : \cos^2\psi = \Omega_0, \tag{3.27}$$

or in another words

$$\cot\Delta = \cot 2b \sin 2c \csc\gamma + \cos 2c \cot\gamma \tag{3.28}$$
$$\cos^2\psi = \sin^2 b \cos^2 c + \cos^2 b \sin^2 c - \frac{1}{2}\sin 2b \sin 2c \cos\gamma, \tag{3.29}$$

where $b = c - a$. The above equations can be envisioned in complex Kerr effect plane as closed loop or in $\psi\Delta$ plane as a contours of fixed compensator azimuth and contours of fixed relative angle between compensator and analyzer (fig. 3.2).

With an ideal quarter wave plate ($\gamma = \frac{\pi}{2}$)

$$\cot\Delta = \cot 2b \sin 2c \tag{3.30}$$
$$\cos^2\psi = \sin^2 b \cos^2 c + \cos^2 b \sin^2 c. \tag{3.31}$$

In the set-up with fixed compensator, linear relations between analyzer and polarizer azimuth and the ellipsometric angles were obtained. This is not the case with the fixed polarizer setup. If we plot ψ against Δ, compensator azimuth corresponds to rotation about the origin at $\Delta = \frac{\pi}{2}, \psi = \frac{\pi}{4}$ and relative angle between analyzer and compensator corresponds to the distance from the origin.

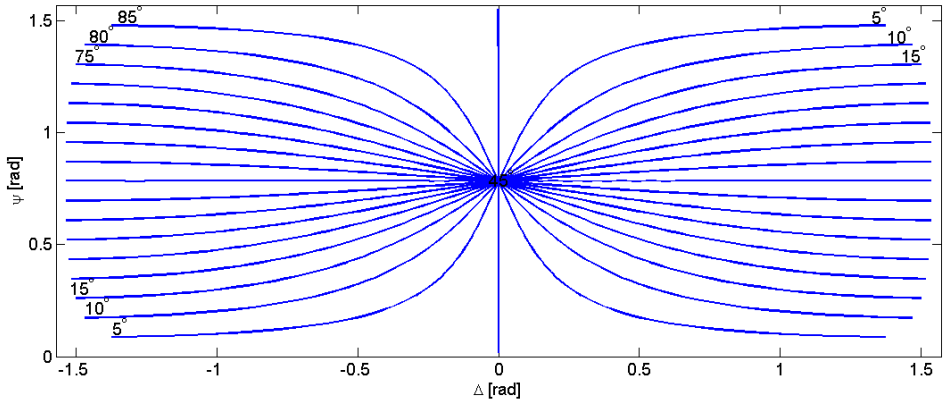

(a) Fixed c contours

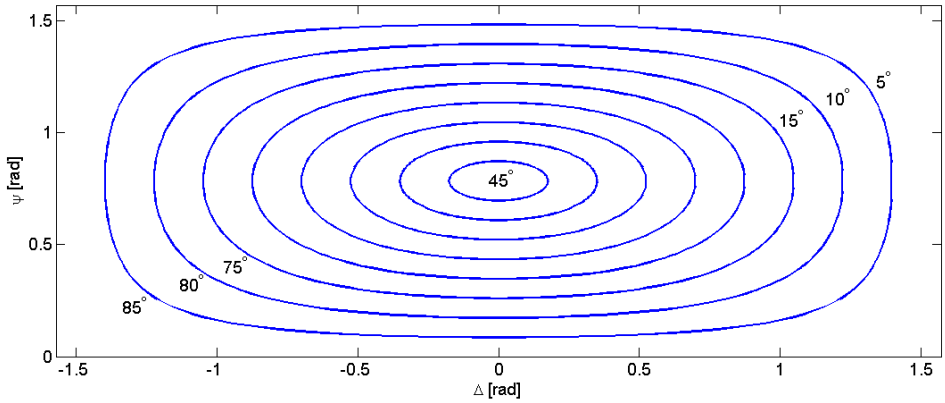

(b) Fixed b contours

Figure 3.2.: Nulling with fixed polarizer

3.2.4. Fixed Modulator, Analyzer and Compensator - Variable Retardation Angle of Compensator

By fixing modulator at $\pm\frac{\pi}{4}$ we can make the second harmonic independent on Δ, and with analyzer fixed at $\pm\frac{\pi}{4}$ and compensator at $\pm\frac{\pi}{8}$ we obtain

$$I_\omega = 0: \quad \tan\Delta = \frac{\sqrt{2}\sin\gamma}{1+\cos\gamma} \tag{3.32}$$

$$I_{2\omega} = 0: \quad \tan\psi = \left(\frac{1-3\cos\gamma}{1+\cos\gamma}\right)^{(\pm)_c(\pm)_a\frac{1}{2}} \tag{3.33}$$

which shows that ellipsometric angles ψ and Δ can also be obtained by alternating the retardation angle of compensator using for example Babinet-Soleil compensator.

Part II.

MOKE Measurements

The magneto-optic Kerr effect (MOKE) has been established as a powerful tool for measuring, with high spatial resolution, all three magnetization components of a magnetic material [FD90]. A polar MOKE configuration can detect the magnetization component perpendicular to the sample surface (out-plane), while the longitudinal and transverse MOKE arrangements measure the two in-plane components.

As already mentioned magneto-optical Kerr effect measurement is significantly improved by adjusting setup to the null position. At the null position equations for the first and the second harmonic signal reduce to

$$\begin{aligned}
\frac{I_\omega}{|r_{ss}|^2 \sin 2(p-m)} &= \tan\psi(\Omega_1(\cos\Delta\epsilon_t + \sin\Delta\theta_t) - \Omega_2(\cos\Delta\theta_t - \sin\Delta\epsilon_t)) \\
&\quad -\Omega_0(\epsilon_s + \tan^2\psi\epsilon_p) + \epsilon_s + \sin 2m\Omega_1 \tan\psi X_2 \\
\frac{I_{2\omega}}{|r_{ss}|^2 \sin 2(p-m)} &= [\tan\psi(\Omega_1(\cos\Delta\theta_t - \sin\Delta\epsilon_t) + \Omega_2(\cos\Delta\epsilon_t + \sin\Delta\theta_t)) \\
&\quad -\Omega_0(\theta_s + \tan^2\psi\theta_p) + \theta_s]\cos 2m + \sin 2m\Omega_1 \tan\psi X_1.
\end{aligned}$$

Thanks to odd parity of sine, the mixed-Kerr-effects coefficients X can be eliminated by zone averaging [PMS+06].

With compensator fixed at 45°, modulator at 0° and polarizer at 45°, taking analyzer angle as positive and $|r_{ss}|^2 = 1$, averaging over two zones with opposite modulator azimuths reduces the above equations to

$$I_\omega = \frac{1}{2}\epsilon_s + \epsilon_t \tan\psi - \frac{1}{2}\epsilon_p \tan^2\psi \tag{3.34}$$

$$I_{2\omega} = \frac{1}{2}\theta_s + \theta_t \tan\psi - \frac{1}{2}\theta_p \tan^2\psi, \tag{3.35}$$

which shows that first harmonic I_ω is proportional to Kerr ellipticity and second harmonic $I_{2\omega}$ is proportional to Kerr rotation at each polarization.

Chapter 4.

Calibration

4.1. Theory

There are various approaches to magneto-optical measurement setup calibration. Calibration methods using oscilloscope, are fast but limited in precision and very demanding on frequency stability. The method suitable for most applications is based on Bessel function properties.

4.2. Rotating analyzer

For polarizer fixed at 45° , modulator at 0° and rotating analyzer we get

$$\mathbf{E_{out}} = \frac{1}{\sqrt{2}} \begin{bmatrix} 1 & 0 \\ 0 & 0 \end{bmatrix} \begin{bmatrix} \cos a & -\sin a \\ \sin a & \cos a \end{bmatrix} \begin{bmatrix} 1 & 0 \\ 0 & \mathrm{e}^{-\mathrm{i}\varphi} \end{bmatrix} \begin{bmatrix} 1 \\ 1 \end{bmatrix}.$$

The intensity at the detector can be calculated as

$$I = \frac{1}{2}\left(1 - \sin 2a \cos\varphi\right). \tag{4.1}$$

Expanding cosine with 3.5

$$\begin{aligned} 2I &= 1 - \sin 2a \\ &\quad [\mathrm{J}_0(\varphi_A)\cos\varphi_0 - 2\mathrm{J}_1(\varphi_A)\sin\varphi_0 \sin\omega t + 2\mathrm{J}_2(\varphi_A)\cos\varphi_0 \cos 2\omega t] \end{aligned}$$

The relation between AC (alternate current) and DC (direct current) components can be obtained in the form:

$$\begin{aligned} \frac{I_{2\omega}}{I_0} &= \frac{-2J_2(\varphi_A)\sin 2a \cos\varphi_0}{1 - J_0(\varphi_A)\sin 2a\cos\varphi_0} \cdot k_{cal} \\ \frac{I_{\omega}}{I_0} &= \frac{2J_1(\varphi_A)\sin 2a \sin\varphi_0}{1 - J_0(\varphi_A)\sin 2a\cos\varphi_0} \cdot k_{cal}, \end{aligned} \tag{4.2}$$

where k_{cal} is calibration parameter.

Setting the PEM retardation angle to the first zero of the Bessel function of the first kind ($\varphi_A = 2.4048$) we can write

$$\frac{I_{2\omega}}{I_0} = 2k_{cal} \cdot J_2(\varphi_A) \sin 2a \cos \varphi_0. \tag{4.3}$$

To check for the linearity of the first harmonic, we write

$$\tan \varphi_0 = \frac{I_\omega}{I_{2\omega}} \frac{J_2(\varphi_A)}{J_1(\varphi_A)} \tag{4.4}$$

for the *residual birefringence* of the PEM. Typical residual birefringence of PEM is around 0.03 rad.

With our PEM based setup, the k_{cal} coefficient was found out to be 0.071deg^{-1} with 650 nm laser. This result in the limits of measurement precision corresponds to the theoretical value of ratio between absolute (DC) and effective (AC) voltage ($\sqrt{2}$).

4.3. Rotating modulator

The Jones matrix of light incident on detector for analyzer fixed at 0 rad is in the form

$$\begin{aligned} \mathbf{E_{out}} = & \frac{1}{\sqrt{2}} \begin{bmatrix} 1 & 0 \\ 0 & 0 \end{bmatrix} \begin{bmatrix} \cos m & -\sin m \\ \sin m & \cos m \end{bmatrix} \\ & \begin{bmatrix} 1 & 0 \\ 0 & \mathrm{e}^{-\mathrm{i}\varphi} \end{bmatrix} \begin{bmatrix} \cos m & \sin m \\ -\sin m & \cos m \end{bmatrix} \begin{bmatrix} 1 \\ 1 \end{bmatrix} \end{aligned} \tag{4.5}$$

The intensity on the detector can be found out to be

$$I = \frac{1}{2} \left(1 + \frac{1}{2} \sin 4m[1 + \cos \varphi] \right). \tag{4.6}$$

For small azimuths of modulator $\sin m \to m$ and we can write

$$2I = 1 + 2m(1 + \cos \varphi) \tag{4.7}$$

Using Bessel function expansion of cosine and $J_0(\varphi_A = 2.4048) = 0$, the relation between ac and dc components can be written as

$$\frac{I_{2\omega}}{I_0} = 4kJ_2(\varphi_A) \frac{m}{1 + 2m}. \tag{4.8}$$

4.4. Application

4.4.1. Spectral calibration method

The zero of the first and the second harmonic corresponds to constant DC signal. This condition can by satisfied by rotating analyzer with any arbitrary voltage applied to PEM. If we plot the first and second harmonic signal and dc signal against the voltage applied to PEM at this point, we obtain three constant functions.

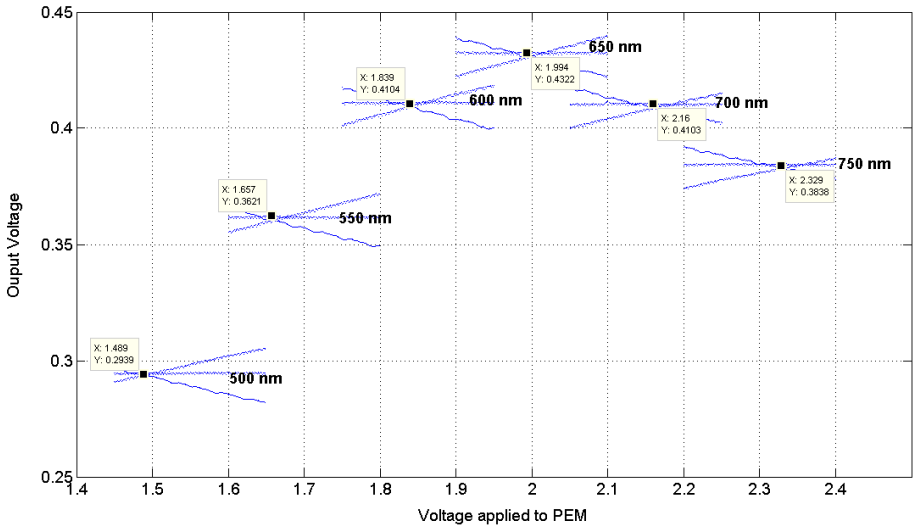

Figure 4.1.: Spectral calibration of PEM

Then the analyzer is rotated to an arbitrary azimuth (lets say 10 degrees from constant position) and the dc signal over the spectrum of voltage applied to PEM is recorded again. The same measurement is then repeated with opposite relative azimuth of analyzer ($-10°$) . The intersect of the three curves is then interpolated. Retardation angle corresponding to voltage applied to PEM at the intersect is 2.405 rad as follows from (4.2).

DC and the second harmonic voltage are then recorded while rotating analyzer back to zero to obtain the calibration parameter k' from the equation 4.8. Parameter k'should be constant over the whole spectrum and serves as a control of the calibration stability.

To speed up the spectral measurement an approximate empiric formula for visible region was found

$$U_{PEM}\left(J_1(2.405) = 0\right) \approx 3.05 \times \lambda[\mu m]\, V, \tag{4.9}$$

for voltage applied to PEM that corresponds to $J_1(2.405) = 0$. For sufficient precision of interpolation measurement for each wavelength is carried out in the 0.2 V interval centered at the approximate value as in figure 4.1 .

Chapter 5.

Simulations - model of magnetic sensor

Yeh formalism was used as a basis for MATLAB program for spectral modeling of planar structures. Some of the results are presented here.

Cobalt/Gold sensor on BK7 glass prism using surface plasmon resonance was optimized for maximum sensitivity to changes in transverse magnetic field. Sensitivity of the sensor is defined here as

$$\frac{\Delta R_p}{R_p} = \frac{R_{p,m+} - R_{p,m-}}{R_{p,0}}, \tag{5.1}$$

where $R_{p,m+}$ ans $R_{p,m+}$ are reflectances in p-polarized light with transverse magnetization in opposite directions and $R_{p,0}$ is reflectance in p-polarized light without magnetization.

The simulated magnetic sensor has following parameters

BK7 prism, permittivity at 632.8nm $\varepsilon \approx 2.310$
Cobalt, permittivity $\varepsilon = -12.5040 + i\,18.4639$, $Q = 0.03273 + i\,0.01092$
Gold, permittivity $\varepsilon = -11.2376 + i\,1.2834$, $Q = 0$
Water, permittivity $\varepsilon \approx 1.775$

where Q is Voigt parameter as defined in (2.8). Ideal dimensions of alternating cobalt and gold layers for highest sensitivity were calculated. Simulations suggest that the highest sensitivity can be achieved with 2.7 nm iron layer. Cobalt is usually preferred for its better stability. Because cover layer with thickness around 1 nm can be difficult to manufacture, an alternative sensor with multiple layers of 2.7 nm thickness is shown.

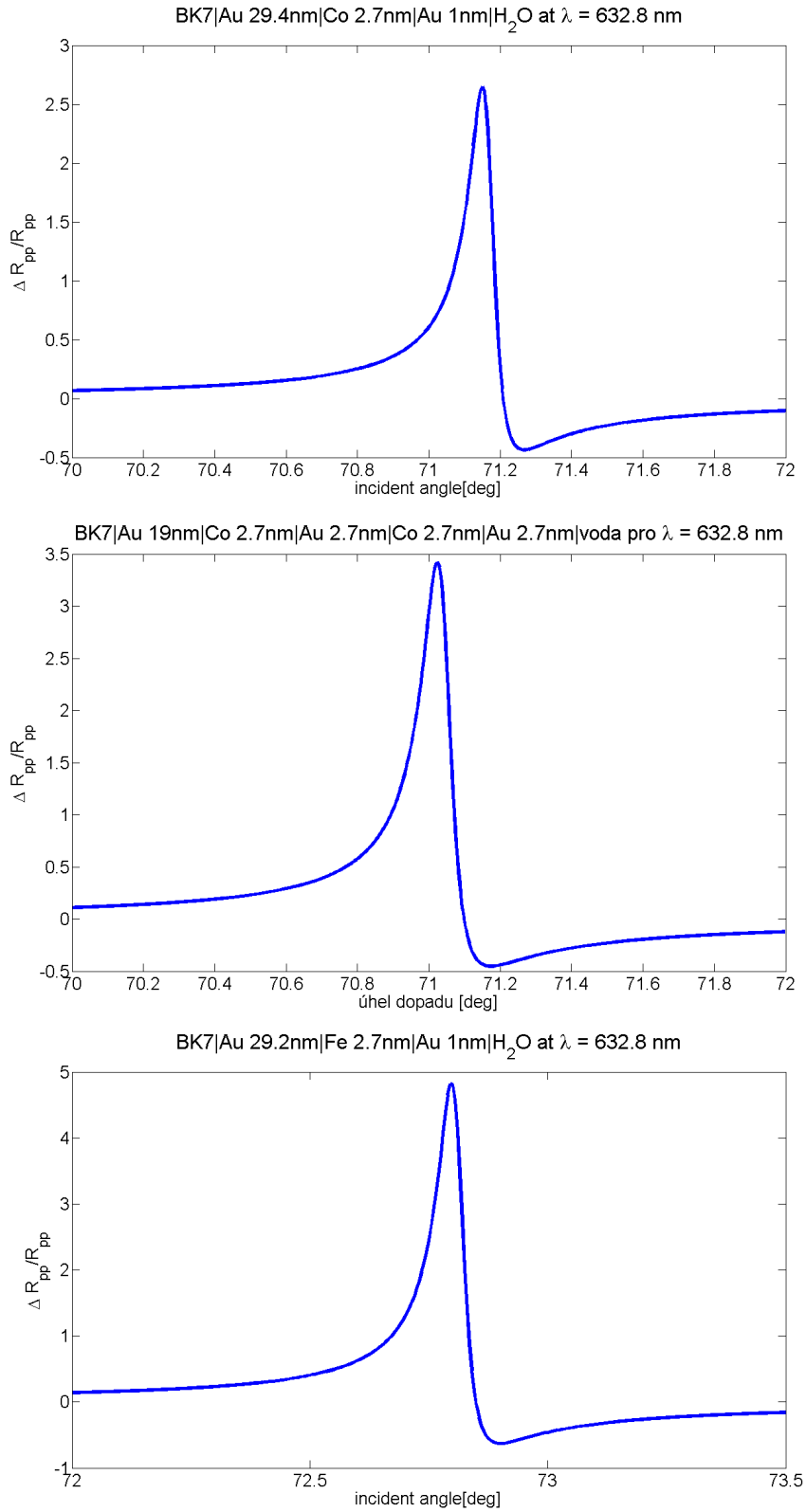

Figure 5.1.: Model of magneto-optical sensor with cobalt and iron magnetic layers

Part III.

Spectral Magneto-optical Measurement Methods

Chapter 6.

Phase Modulation Method

Signal to noise ratio (SNR) is direct measure of modulation method quality. Possible modulation techniques can be therefore compared by comparing their SNR. Photonic noise is calculated here as it is the only irreducible part of noise introduced to measurement.

With modulator fixed at 45° relative to polarizer, the Jones matrix equation of the system becomes:

$$\begin{aligned}\mathbb{E} = &\begin{bmatrix} \cos^2 a & \sin a\,\cos a \\ \sin a\,\cos a & \sin^2 a \end{bmatrix} \begin{bmatrix} r_{ss} & r_{sp} \\ r_{ps} & r_{pp} \end{bmatrix} \\ &\begin{bmatrix} e^{i\frac{\varphi}{2}} & 0 \\ 0 & e^{-i\frac{\varphi}{2}} \end{bmatrix} \begin{bmatrix} \cos p \\ \sin p \end{bmatrix} \\ &= \begin{bmatrix} \cos^2 a(r_{ss}e^{i\frac{\varphi}{2}}\cos p + r_{sp}e^{-i\frac{\varphi}{2}}\sin p) \\ \sin^2 a(r_{ps}e^{i\frac{\varphi}{2}}\cos p + r_{pp}e^{-i\frac{\varphi}{2}}\sin p) \end{bmatrix} \end{aligned} \tag{6.1}$$

From electric field we can calculate intensity of p-polarized light

$$\begin{aligned} 2I_{p,a=\frac{\pi}{2}} &= \mathbb{E}^\dagger\mathbb{E} = |r_{ps}|^2\cos^2 p + |r_{pp}|^2\sin^2 p + (r_{ps}r_{pp}^* e^{i\varphi} + r_{ps}^* r_{pp}e^{-i\varphi})\sin p\cos p \\ 2I_p &\approx |r_{pp}|^2\left[(\theta_p^2+\epsilon_p^2)\cos^2 p + \sin^2 p + \Re\left\{\frac{r_{ps}}{r_{pp}}e^{i\varphi}\right\}\sin 2p\right] \\ &\approx |r_{pp}|^2\left[\sin^2 p - \theta_p\sin 2p\cos\varphi + \epsilon_p\sin 2p\sin\varphi\right] \end{aligned}$$

Signal-to-noise ratio is defined the ratio of the part of intensity that carries the measured signal (in this case first harmonic signal $I_\omega$and second harmonic signal $I_{2\omega}$) to square root of the remaining part of the intensity (I_0).

$$\begin{aligned}\frac{I_\omega}{\sqrt{I_0}} &\approx |r_{pp}| I_{in} \frac{\sin 2p}{\sin p} 4J_1(\varphi_A)\epsilon_p \approx \epsilon_p \cos p \\ \frac{I_{2\omega}}{\sqrt{I_0}} &\approx -|r_{pp}| I_{in} \frac{\sin 2p}{\sqrt{\sin^2 p - \theta_p \sin 2p}} 4J_2(\varphi_A)\theta_p \approx -0.863\theta_p \cos p \end{aligned} \quad (6.2)$$

a...analyzer azimuth
p...polarizer azimuth (set to 45° by default)
φ...retardation introduced by PEM
$\frac{r_{ps}}{r_{pp}} = -\chi_p = -\theta_p - i\epsilon_p$ ...complex Kerr effect in p-polarized light
$\varphi = \varphi_0 + \varphi_A \sin \omega\tau$ ...phase retardation introduced by PEM
φ_0...residual birefringence (ideally zero)
φ_A...amplitude of modulation (set to 2.405 rad by calibration)
I_{in}...intensity of incident light
I_p...intensity of p-polarized light
$J_1(\varphi_A)$...value of Bessel function of the first kind at φ_A
θ_p...Kerr rotation in p-polarized light
ϵ_p...Kerr ellipticity in p-polarized light

Detecting second harmonic signal we get following results

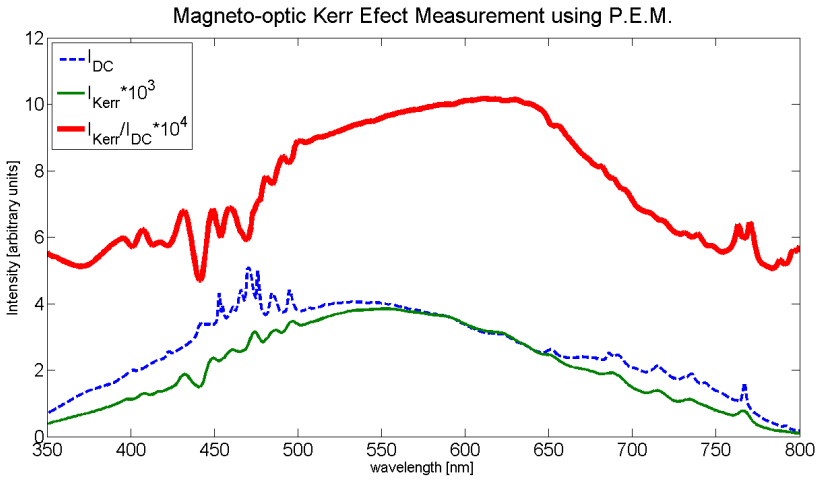

Figure 6.1.: Spectral measurement of Kerr rotation in transverse magnetization with phase modulation

Chapter 7.

Azimuth Modulation Method

Alternate current applied to a coil with glass core generates magnetic field that periodically changes polarization of propagating light due to Faraday effect (fig. 7.1).

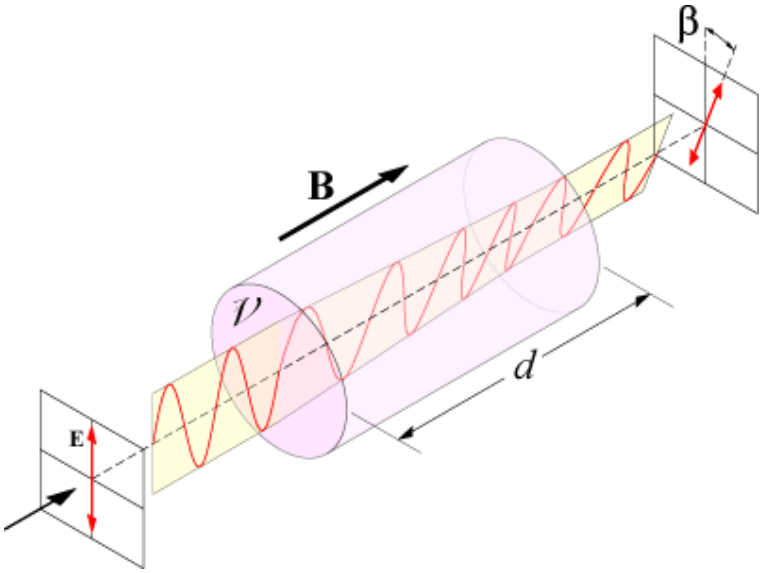

Figure 7.1.: Faraday effect, d is length of the coil core in meters, **B** is magnetic flux density in the direction of propagation in Teslas, β is Faraday rotation in radians, $\mathcal{V}$ is Verdet constant of material. Angle of rotation of the polarization $\beta = B\mathcal{V}d$.

Using Faraday Cells as Modulator and Nullator the Jones matrix equation of the

setup becomes:

$$\mathbb{E} = \begin{bmatrix} \cos^2 a & \sin a \cos a \\ \sin a \cos a & \sin^2 a \end{bmatrix} \begin{bmatrix} r_{ss} & r_{sp} \\ r_{ps} & r_{pp} \end{bmatrix} \begin{bmatrix} e^{i\frac{\delta}{2}} & 0 \\ 0 & e^{-i\frac{\delta}{2}} \end{bmatrix} \begin{bmatrix} \cos(\eta + \beta_0 \sin \omega t) & -\sin(\eta + \beta_0 \sin \omega t) \\ \sin(\eta + \beta_0 \sin \omega t) & \cos(\eta + \beta_0 \sin \omega t) \end{bmatrix} \begin{bmatrix} \cos p \\ \sin p \end{bmatrix} = \begin{bmatrix} \cos^2 a (r_{ss} e^{i\frac{\delta}{2}} \cos \Omega + r_{sp} e^{-i\frac{\delta}{2}} \sin \Omega) \\ \sin^2 a (r_{ps} e^{i\frac{\delta}{2}} \cos \Omega + r_{pp} e^{-i\frac{\delta}{2}} \sin \Omega) \end{bmatrix} \quad (7.1)$$

From electric field we can calculate intensity of p-polarized light

$$\begin{aligned} 2I_p &= \mathbb{E}^\dagger \mathbb{E} = |r_{ps}|^2 \cos^2 \Omega + |r_{pp}|^2 \sin^2 \Omega + (r_{ps} r_{pp}^* e^{i\delta} + r_{ps}^* r_{pp} e^{-i\delta}) \sin \Omega \cos \Omega \\ 2I_p &\approx |r_{pp}|^2 \left[\frac{|r_{ps}|^2}{|r_{pp}|^2} \cos^2 \Omega + \sin^2 \Omega + Re \left\{ \frac{r_{ps}}{r_{pp}} e^{i\delta} \right\} 2 \sin \Omega \cos \Omega \right] \\ &\approx |r_{pp}|^2 \left[(\theta_p^2 + \epsilon_p^2) \cos^2 \Omega + \sin^2 \Omega - \theta_p \cos \delta \sin 2\Omega + \epsilon_p \sin \delta \sin 2\Omega \right] \end{aligned}$$

Signal-to-noise ratio is defined the ratio of the part of intensity that carries the measured signal (in this case first harmonic signal I_ω) to square root of the remaining part of the intensity (I_0).

$$\frac{I_\omega}{\sqrt{I}} \approx I_{in} |r_{pp}| \frac{\theta_p \sin 2\beta_0}{\sqrt{\sin p - \theta_p \sin 2p + \theta_p^2 \cos^2 p}} \approx [p \to 0] \approx \sin 2\beta_0 \quad (7.2)$$

a...azimuth of analyzer (a=$\frac{\pi}{2}$for p-polarized light, a=0 for s-polarized light)
δ...phase-plate or compensator phase shift
η...azimuth of compensating Faraday cell
ω...modulation frequency of Faraday cell
β_0...amplitude of Faraday cell azimuth modulation (approx. 3°)
p...polarizer azimuth (p=0 for p-polarized light detection, p=$-\frac{\pi}{2}$for s-polarized light)
$\Omega = p + \eta + \beta_0 \sin \omega t$

SNR ratio of compared methods is

$$\frac{SNR_{phase}}{SNR_{azimuth}} = \frac{0.863 \theta_p \cos p}{\sin 2\beta_0} \approx 6\theta_p \quad (7.3)$$

taking polarizer azimuth in PMSA setup $p = 45^\circ$ and amplitude of Faraday cell modulation in PMCSA setup $\beta_0 = 3^\circ$. Having shown that amplitude modulation technique SNR is virtually independent of measured Kerr effect we can conclude that it is more suitable for measurement of Kerr effects that are usually in the range of miliradians.

Chapter 8.

Amplitude Modulation Method

Amplitude modulation technique uses an instrument called chopper that periodically inhibits incident light. This was an early modulation technique that was later surpassed by photo-elastic modulation that offers orders of magnitude better signal to noise ratio. On the plus side, chopper unlike PEM does not require any kind of calibration.

Comparison of phase and amplitude modulation stability (8.1)

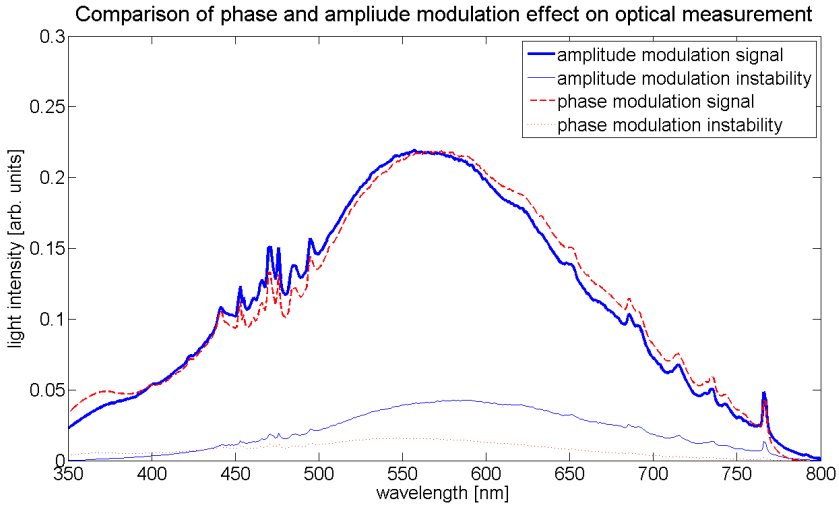

Figure 8.1.: Optical spectra measured using phase modulation and amplitude modulation

The apparent difference between optical signal detected with phase modulation and with amplitude modulation shows the mentioned need for photo-elastic modulator calibration. In this measurement the PEM is not calibrated and therefore introduces slightly different retardation to each wavelength deforming the measured function.

Part IV.

Summary

8.1. Conclusions

General equations of ellipsometric measurement that allow quick insight into each Kerr effect measurement setup advantages and limitations are introduced here. Using these equations an alternative nulling procedure for Kerr Effect measurement was calculated and tested successfully.

Irreducible noise calculations for various approaches to MOKE measurement were carried out. Based on these calculations, two methods were picked for application. Method with photo-elastic modulation and Faraday compensation cell and with both modulation and compensation Faraday cells. Second method promises better signal to noise ratio. The only drawback is bigger demand for ambient light and mechanical vibration cancellation.

Yeh formalism based program for spectral magnetic anisotropic planar structures modeling was developed and applied for various magnetic detector designs.

8.2. Further Development

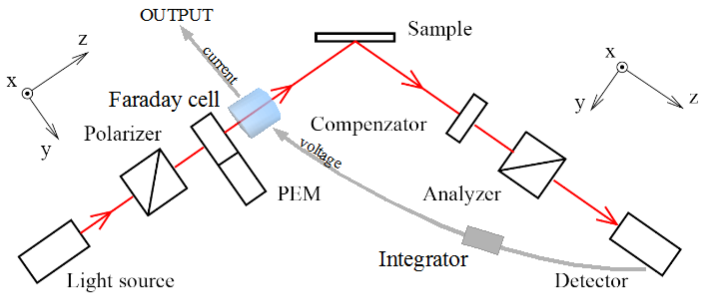

Figure 8.2.: Kerr effect measurement setup with Faraday compensation cell and photo-elastic modulation

Spectral magneto optical measurement setup with phase modulation and Faraday compensation cell for VŠB-TUO Both phase and azimuth modulation techniques with Faraday compensation cell are being applied in spectral magneto-optical measurement setup currently developed at VŠB-TUO. The setup was already successfully tested with phase modulation and direct data acquisition. First tests of azimuth modulation cell were carried out that conformed the anticipated issue of cell overheating at desirable modulation frequencies and

currents generating the intended 3° amplitude of modulation. New Faraday modulation cell is being designed that should overcome this problem.

The author of this work suggest that Faraday compensation cell is introduced to the setup. With this approach, the signal is measured indirectly as the current through compensation cell that is controlled by feedback from nulled detector.

The topic has been chosen for PhD. thesis that should further develop ideas presented in this work:

SNOM based MOKE measurement setup at ICMAB, Barcelona SNOM (Scanning near-field optical microscopy) uses a sharpened optical fiber tip as a sub-wavelength light source or detector to probe the optical field distribution in the vicinity to the sample surface. In the case of magneto-optical measurements with SNOM, the polarization state of the signal should be analyzed to achieve magneto-optical contrast. This technique has the advantage of providing a simultaneous measurement of the sample's topography that can prove invaluable in eliminating topographic artifacts from the magneto-optical data.

Illumination is provided by a laser in both transmission and reflection modes. Polarization of the illuminating light is controlled using a half-wave plate. Light transmitted through or reflected from the sample is collected by a sharpened optical fiber probe and, after decoupling, sent through a polarizer onto the detector. For polarization measurements, uncoated chemically etched fiber tips are used in order to avoid the depolarization effects associated with metal-coated SNOM tips.

Although spatial resolution provided with uncoated fiber tips is less than that achievable with metal coated tips, the advantages of polarization measurements are much more significant for magneto-optical studies. Uncoated SNOM fiber tips have larger optical acceptance area than the metal coated tips, however they still provide sub-wavelength resolution since they probe the evanescent fields present in the near-field region close to the surface. In addition, polarization analysis combined with SNOM measurements greatly improves the contrast and resolution obtained with uncoated fiber tips.

Bibliography

[AB87] R. M. A. Azzam and N. M. Bashara. *Ellipsometry and Polarized Light*. North-Holland, Amsterdam, 2nd edition, 1987.

[BBF+88] M. N. Baibich, J. M. Broto, A. Fert, F. N. Van Dau, F. Petroff, P. Eitenne, G. Creuzet, A. Friederich, and J. Chazelas. Giant magnetoresistance of (001)fe/(001)cr magnetic superlattices. *Phys. Rev. Lett.*, 61:2472–2475, 1988.

[BW75] M. Born and E. Wolf. *Principles of Optics*. Pergamon, Oxford, 5th edition, 1975.

[Dax97] M. Dax. The nonvolatile memory challenge. *Semiconduct. Int.*, 20:84–89, 1997.

[FD90] J. M. Florczak and E. D. Dahlberg. Detecting two magnetization components by the magneto-optical kerr effect. *J. Appl. Phys*, 67:7520–7525, 1990.

[PMS+06] K. Postava, A. Maziewski, A. Stupakiewicz, A. Wawro, L. T. Baczewski, Š. Višňovský, and T. Yamaguchi. Transverse magneto-optical kerr effect measured using phase modulation. *Journal of the European Optical Society*, 06017:8, October 2006.

[PMY+04] K. Postava, A. Mazievsky, T. Yamaguchi, R. Ossikovski, Š. Višňovský, and J. Pištora. Null ellipsometer with phase modulation. *OSA*, 12(24):6, November 2004.

[ST95] B. E. A. Saleh and M. C. Teich. *Základy fotoniky*. MATFYZPRESS, 1995.

[WAB+01] S. A. Wolf, D. D. Awschalom, R. A. Buhrman, J. M. Daughton, S. von Molnár, M. L. Roukes, A. Y. Chtchelkanova, and D. M. Treger. Spintronics: A spin-based electronics vision for the future. *Science*, 294:1488–1495, 2001.

[Yeh80] Pochi Yeh. Optics of anisotropic layered media: A new 4×4 matrix algebra. *Surf. Sci.*, 96:41–53, 1980.

[YY84] A. Yariv and P. Yeh. *Optical Waves in Crystals*. John Wiley & Sons, London, 1984.